*Erschienen in: Physica Status Solidi (A) - Applications and Materials Science ; 215 (2018), 24. - 1800741*
*https://dx.doi.org/10.1002/pssa.201800741*

# Bulk and Surface-Related Degradation in Lifetime Samples Made of Czochralski Silicon Passivated by Plasma-Enhanced Chemical Vapor Deposited Layer Stacks

*David Sperber,* Anton Schwarz, Axel Herguth, and Giso Hahn*

**Significant bulk-related degradation (BRD) is followed by surface-related degradation (SRD) of effective excess charge carrier lifetime in lifetime samples made of Czochralski silicon during illuminated treatment at 80–150 °C. Samples are passivated with either $AlO_x$:H/$SiO_xN_y$:H/$SiN_x$:H or $SiO_xN_y$:H/$SiN_x$:H stacks stemming entirely from plasma-enhanced chemical vapor deposition. Samples show strong variations in BRD depending on passivation stacks and treatment conditions, and a potential link to light and elevated temperature-induced degradation (LeTID) is discussed. All samples are fired in a belt furnace, and variations of firing temperature and belt speed are shown to influence SRD slightly. SRD is furthermore accelerated with increasing treatment temperature and an apparent activation energy $E_{app} = 1.07 \pm 0.02$ eV is determined in $SiO_xN_y$:H/$SiN_x$:H passivated samples. Interpretation of $E_{app}$ is, however, difficult as both changes in interfacial defect and fixed charge density occur in parallel during SRD.**

## 1. Introduction

Light-induced degradation (LID) may severely limit effective excess charge carrier lifetime $\tau_{eff}$ in crystalline silicon and result in lowered efficiency of affected solar cells. Quite a few different phenomena leading to LID have been observed, as described, e.g., by Lindroos and Savin.[1] Monocrystalline silicon grown by the Czochralski method (Cz-Si) is known for a long time to be affected by light-induced formation of boron–oxygen complexes (BO-LID)[2–6] and occasionally by iron–boron (FeB) pair association and dissociation.[7–9] Recently, it was proposed that light and elevated temperature-induced degradation (LeTID), first discovered in multicrystalline silicon,[10–12] is possibly affecting Cz-Si, too.[13–15]

D. Sperber, A. Schwarz, A. Herguth, Prof. G. Hahn
Department of Physics
University of Konstanz
Universitätsstr. 10, 78464 Konstanz, Germany
E-mail: david.sperber@uni-konstanz.de

While in these bulk-related degradation (BRD) phenomena the bulk excess charge carrier lifetime $\tau_b$ of a sample is susceptible to light-induced changes, recent research results showed that the passivation quality of layers/stacks comprising hydrogen-rich silicon nitride ($SiN_x$:H) can degrade and recover under illumination and temperature treatment as well as after a fast firing step as used for contact formation in solar cell production.[16] This surface-related degradation (SRD) appears to be a carrier-induced effect[17] and is not related to UV photons which may cause degradation of surface passivation, too.[18] Samples with a highly doped region at the surface (forming an emitter or a high-low junction) have been found to be less affected by SRD.[15,17] The rear surface of most passivated emitter and rear cells (PERC),[19] however, does not feature such a highly doped region underneath the passivation layer and might therefore be susceptible to SRD. Indeed, solar cells with $SiO_x$/$SiN_x$:H rear side passivation were recently found to be affected by significant SRD during illuminated treatment at 150 °C.[20]

In this study, we investigate BRD and SRD in lifetime samples made of Czochralski silicon (Cz-Si) without highly doped surface and passivation stacks deposited entirely by plasma-enhanced chemical vapor deposition (PECVD) thus resembling a PERC rear side passivation. Furthermore, a series of degradation treatments at different temperatures allows for a quantitative analysis of degradation kinetics by determining an apparent activation energy of SRD in samples passivated with $SiO_xN_y$:H/$SiN_x$:H.

## 2. Experimental Section

Lifetime samples were made of boron-doped (2 Ω cm; $N_d \approx 7 \times 10^{15}$ cm$^{-3}$) Cz-Si wafers of edge length 156 mm and initial thickness ≈200 µm. The wafers received a saw damage etch in an aqueous solution of potassium hydroxide (22%, 80 °C) leading to a thickness of ≈180 µm followed by a 30 s chemical polishing step at room temperature in a solution of nitric acid (65%), acetic acid (99.8%), and hydrofluoric acid (50%) mixed in a ratio 29:5:3. To remove impurities, the surface of the samples

was oxidized at 80 °C in a solution of hydrogen peroxide (30%) and sulphuric acid (96%) mixed in a ratio 1:3 followed by a dip in diluted hydrofluoric acid (2%).

Wafers were then coated entirely in an industrial direct plasma PECVD tool working at 40 kHz. Part of the wafers received a thin silicon oxy-nitride ($SiO_xN_y$:H) coating (≈25 nm, refractive index $n_{600}$ ≈1.6) capped by ≈120 nm $SiN_x$:H ($n_{600}$ ≈2.0). Other wafers received a stack consisting of ≈10 nm aluminum oxide ($AlO_x$:H) followed by ≈10 nm $SiO_xN_y$:H and ≈120 nm $SiN_x$:H. All layers were deposited symmetrically on both wafer sides. Afterwards, wafers were laser-cut to square-sized samples of 5 cm edge length and fired in an industrial fast firing belt furnace (Centrotherm c.FIRE 8.400–300 L) at belt speed 6 m min$^{-1}$ and measured peak sample temperature ≈800 °C if not stated otherwise. After firing, samples were stored in darkness until measurement series started.

During measurement series, samples were treated on hotplates held at constant temperature in ambient air. At the same time, samples were exposed to halogen lamp illumination of ≈1 sun equivalent intensity (abbreviated "suns"),[21] realized by matching the short circuit current of a solar cell to that under a solar spectrum simulator. Treatment was repeatedly interrupted for measurement of the effective excess charge carrier lifetime $\tau_{eff}$ in dependence of excess charge carrier density $\Delta n$ using a Sinton Instruments lifetime tester (WCT-120) at 30 °C.[22] The extent of degradation was quantified with the change in effective defect density $\Delta N_{eff}(t)$ after an accumulated treatment time $t$

$$\Delta N_{eff}(t) = \frac{1}{\tau_{eff}(t)} - \frac{1}{\tau_{eff}(t_0)} \quad (1)$$

To experimentally determine the quality of surface passivation, the surface-related saturation current density $J_{0s}$[23] was calculated according to the method described by Kimmerle et al.[24] as applied for characterization of SRD before.[16] The fit range of $\Delta n$ for determination of $J_{0s}$ was set from $5\times10^{15}$ to $1\times10^{16}$ cm$^{-3}$. Capacitance–voltage ($C$–$V$) measurements yielding the fixed charge density $Q$ of dielectric layers were carried out using a mercury probe on the sample side which was illuminated during LID treatment. To estimate an uncertainty of measured $Q$ due to repeated contacting at roughly the same sample spot, another sample was not treated at LID conditions but was repeatedly contacted, and resulting variations are shown as uncertainty of measured $Q$.

## 3. Results and Discussion

### 3.1. $AlO_x$:H/$SiO_xN_y$:H/$SiN_x$:H Passivated Samples

In **Figure 1**, measurement data of a boron-doped Cz-Si sample passivated with an $AlO_x$:H/$SiO_xN_y$:H/$SiN_x$:H stack and fired at 800 °C are shown during treatment at 80 or 150 °C and ≈1 sun resembling accelerated aging conditions. The sample treated at 80 °C shows a strong decline of $\tau_{eff}$ leading to minimum I and a subsequent recovery leading to maximum II after ≈50 h of treatment due to very strong BRD with degradation of $\tau_{eff}$ strongest at lower excess carrier densities $\Delta n$ (data not shown). The origin of such strong BRD will be discussed later on. In fact, even the residual influence of BRD at higher $\Delta n$ prevents proper extraction of $J_{0s}$ during the first hours of treatment.

For treatment times exceeding ≈50 h, degradation of $\tau_{eff}$ can be observed and is accompanied by rising $J_{0s}$. This increase of $J_{0s}$ indicates (as discussed in more detail elsewhere[16]) that the long-term degradation of $\tau_{eff}$ results from deterioration of surface passivation quality and supports the conclusion that the PECVD-deposited $AlO_x$:H/$SiO_xN_y$:H/$SiN_x$:H passivation stack is affected by significant SRD. It should be noted that earlier studies which investigated fired lab-type stacks comprising $AlO_x$:H made by atomic layer deposition (ALD) and capped with PECVD $SiN_x$:H observed much higher stability of passivation quality during similar treatments.[15,17,18,26]

Treating another sample at an increased temperature of 150 °C (Figure 1, right) accelerates the curve progression with similar features I and II. Additionally, it can now be seen that the sample shows a recovery after reaching a minimum III of $\tau_{eff}$ after ≈100 h of treatment. It was observed before that degradation of $AlO_x$:H/$SiN_x$:H stacks at 150 °C is mainly caused by loss of fixed charge density $Q$, and quantitative determination of $J_{0s}$ in that kind of samples has proven unreliable at elevated temperatures.[17] For the treatment at 150 °C shown in Figure 1, $J_{0s}$ analysis fails, too, during the decline toward minimum III,

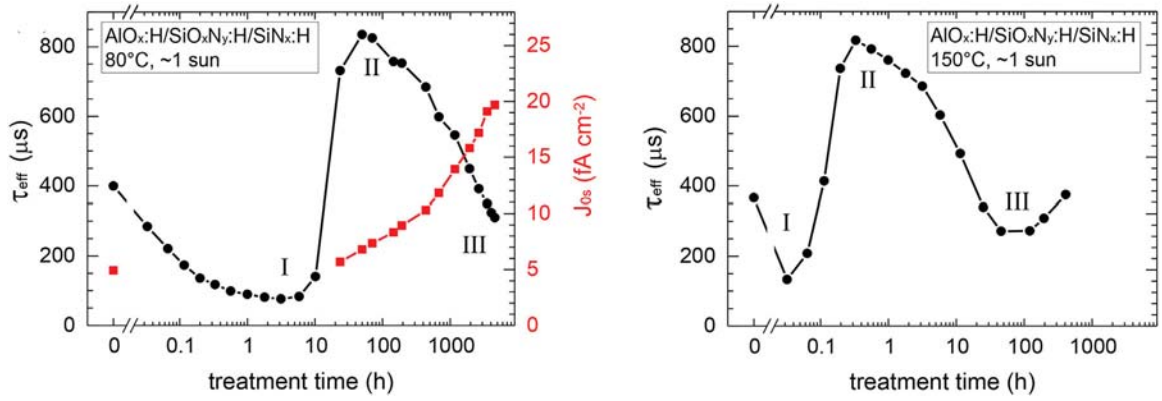


**Figure 1.** Measurement of effective lifetime $\tau_{eff}$ ($\Delta n = 0.1 \cdot N_d$) and $J_{0s}$ of Cz-Si samples passivated with an $AlO_x$:H/$SiO_xN_y$:H/$SiN_x$:H stack during treatment at ≈1 sun and either 80 °C (left) or 150 °C (right). Part of data taken from Ref. [25].

and $\tau_{eff}$ at higher $\Delta n$ surpasses $\tau_{eff}$ at lower $\Delta n$ after ≈15 h of treatment (data not shown) which is suspected to result from loss of $Q$.[17] Owing to the complex sample structure and difficult $J_{0s}$ extraction, further SRD analysis has not been carried out for $AlO_x$:H/$SiO_xN_y$:H/$SiN_x$:H samples.

### 3.2. $SiO_xN_y$:H/$SiN_x$:H Passivated Samples

Besides $AlO_x$:H, silicon oxy-nitride ($SiO_xN_y$:H) can be used as passivating layer underneath a $SiN_x$:H capping. **Figure 2** shows measurement data of samples passivated with a $SiO_xN_y$:H/$SiN_x$:H stack during treatment at ≈1 sun and temperatures of 80 or 150 °C.

Treatment at 80 °C leads to a minimum (I) in $\tau_{eff}$ after ≈1 h while $J_{0s}$ shows no significant change during that time, indicating BRD. Compared to Figure 1, the extent of degradation is less pronounced in minimum (I) and recovery occurs faster. After regeneration of BRD, the following decline of $\tau_{eff}$ toward minimum III is accompanied by rising $J_{0s}$ and can therefore be explained by degradation of surface passivation quality. Like single PECVD $SiN_x$:H passivation layers[16] and stacks comprising an $AlO_x$:H interlayer, a PECVD $SiO_xN_y$:H/$SiN_x$:H stack may obviously suffer from SRD as well. Treatment at 150 °C accelerates this process (Figure 2, right): SRD can be observed already after ≈30 min of treatment compared to ≈20 h at 80 °C. The underlying defect formation mechanism can therefore be presumed to be thermally activated and an apparent activation energy will be determined later on.

### 3.3. LeTID in Czochralski Silicon

According to Figure 1 and 2, the extent of BRD is much less pronounced and regeneration occurs faster in $SiO_xN_y$:H/$SiN_x$:H samples compared to $AlO_x$:H/$SiO_xN_y$:H/$SiN_x$:H samples. As it is expectable that neither the extent of BO-LID in samples of same base material differs that much nor that regeneration speeds up, a possible explanation is that different dielectric passivation stacks lead to differing strength of LeTID in Cz-Si similar to earlier observations in mc-Si.[27]

To further investigate this hypothesis, additional samples were treated at either 32 °C and ≈0.1 suns or at 80 °C and ≈1 sun as shown in **Figure 3**. The first measurement after treatment start was chosen as point of reference $t_0$ for calculation of $\Delta N_{eff}$ to exclude an influence of initial illumination effects such as FeB dissociation[7–9] which likely causes the initial rise of $\tau_{eff}$ observed in three of the four samples. Afterwards, treatment at 32 °C should lead to little or very slow LeTID which has been shown to occur very slowly even at 50 °C in mc-Si.[28] Comparing the maximal change in effective defect density $\Delta N_{eff}$ of the differently treated samples shows that, indeed, degradation changes significantly depending on degradation conditions.

The differently passivated samples show a rather similar degradation at 32 °C up to ≈20 h. While the $SiO_xN_y$:H/$SiN_x$:H sample shows a saturating behavior after less than 100 h of treatment as would be expected due to BO-LID, the $AlO_x$:H/$SiO_xN_y$:H/$SiN_x$:H sample shows a continued long-term degradation which cannot be explained by BO-LID and indicates an additional degradation mechanism. Additionally, it can be seen that degradation is apparently weaker for a $SiO_xN_y$:H/$SiN_x$:H sample treated at 80 °C compared to treatment at 32 °C because BO-related regeneration sets in earlier. Degradation of an $AlO_x$:H/$SiO_xN_y$:H/$SiN_x$:H sample, on the other hand, is much stronger at 80 °C compared to 32 °C at least up to several hundred hours of treatment in agreement with the hypothesis of additional LeTID in these samples which is very slow at 32 °C and thus far from saturation at the end of treatment at 32 °C.

In addition to these observations, it has been shown before that $\Delta N_{eff}$ increases strongly with increasing firing temperature in the same Cz-Si material[15] which is a known property of LeTID in mc-Si as well.[29,30] Taken together, the dependency on choice of passivation layers, firing temperature and treatment conditions make it very likely that LeTID may affect Cz-Si in addition to BO-LID.

### 3.4. Further Investigation of SRD

**Figure 4** shows the influence of firing step parameters on subsequent SRD. As can be seen, different belt speeds all lead to significant SRD in samples fired at 800 °C and variations in

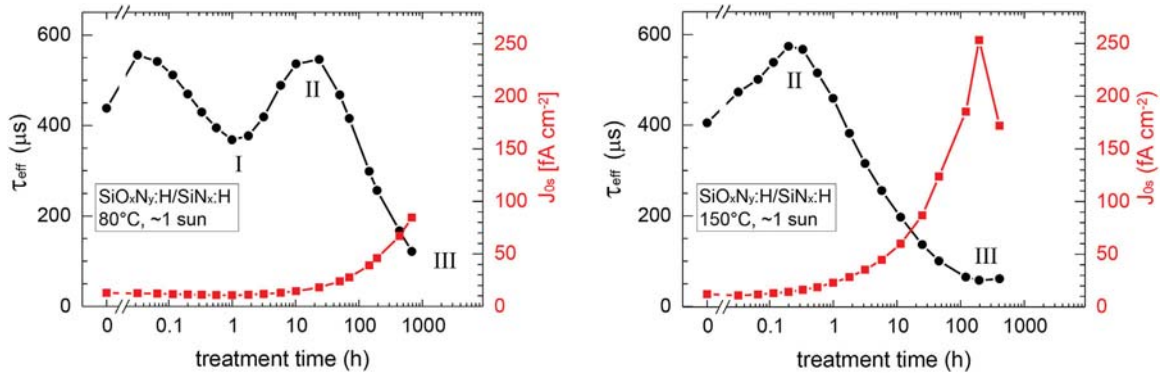


**Figure 2.** Measurement of $\tau_{eff}$ ($\Delta n = 0.1\,N_d$) and $J_{0s}$ of Cz-Si samples passivated with a $SiO_xN_y$:H/$SiN_x$:H stack during treatment at ≈1 sun and either 80 °C (left) or 150 °C (right). Part of data taken from Ref. [25].

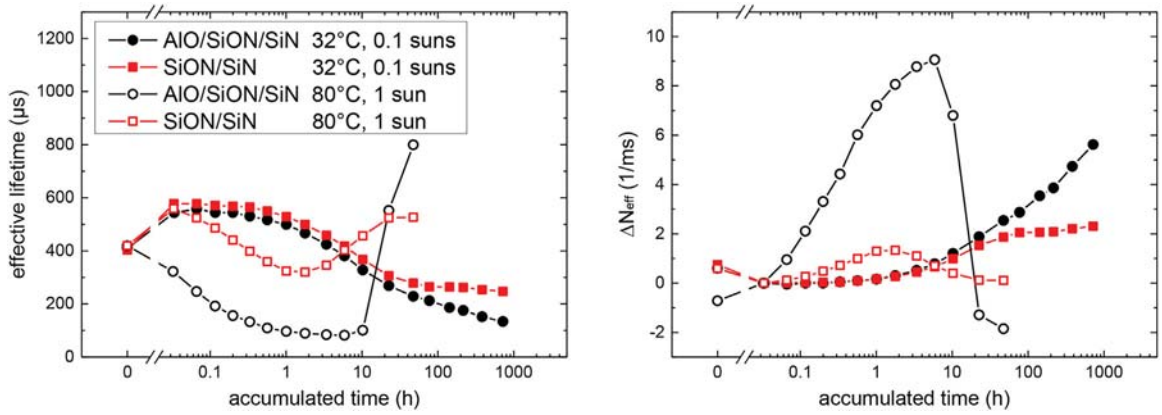


**Figure 3.** Measurement of (left) $\tau_{eff}$ ($\Delta n = 0.1 \cdot N_d$) and (right) $\Delta N_{eff}$ of differently passivated Cz-Si samples during treatment at either ≈0.1 suns and 32 °C or ≈1 sun and 80 °C.

degradation behavior remain modest. Only after prolonged treatment, a stronger increase of $J_{0s}$ can be observed in samples fired at higher belt speed. A change in peak firing temperature while keeping the belt speed constant at 6 m min$^{-1}$ results in more pronounced changes in degradation behavior: samples fired at higher temperature start at lower $J_{0s}$ but degrade stronger and/or faster. Additionally, the sample fired at 850 °C reaches a plateau in $J_{0s}$ before 100 h of treatment while the other samples show no saturating behavior up to this point. In summary, it can be stated that samples fired at belt speeds ranging from 4 to 7 m min$^{-1}$ and at measured peak firing temperatures ranging from 700 to 850 °C are all affected by significant SRD.

Determining an activation energy is considered helpful to better understand the characteristics of SRD and predict its appearance. This was done according to an empirical approach which is discussed in more detail later on. First, a change in effective interfacial defect concentration $\Delta N_{eff}$ is calculated from effective lifetime data according to Equation (1) which is a known procedure for bulk defects. $\Delta N_{eff}$ is found to resemble the shape of a single exponential saturating growth curve

$$\Delta N_{eff}(t) = \Delta N_{sat}\{1 - \exp[-k_{app}(t - t_0)]\} \quad (2)$$

yielding a saturation value $\Delta N_{sat}$ and an apparent reaction rate $k_{app}$ which was determined for treatments at five different temperatures $T$ (two samples each). **Figure 5** shows an example.

Assuming that the probability of a single defect to form is proportional to the availability of phonons with energy in excess of a certain activation energy, the correlated reaction constant $k$ is proportional to the Boltzmann factor comparing mean thermal energy $k_B T$ and activation energy $E_a$

$$k(T) = k_0 \exp\left(-\frac{E_a}{k_B T}\right) \quad (3)$$

with $k_0$ being a characteristic trial frequency. The above relation (3) is known as Arrhenius law and can be used to determine an activation energy $E_a$.

The obtained degradation rates $k_{app}(T)$ are shown in an Arrhenius plot in **Figure 6**. A fit using Equation (3) yields an apparent activation energy of $E_{app} = 1.07 \pm 0.02$ eV for the

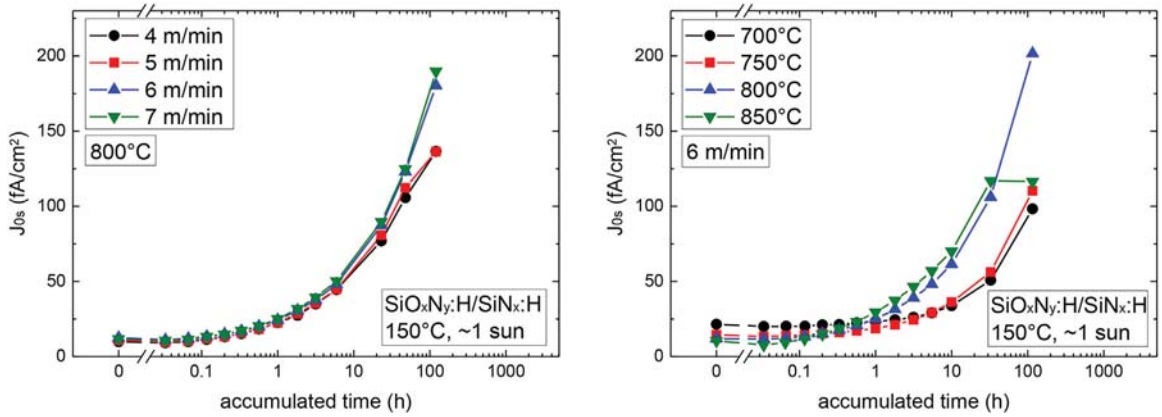


**Figure 4.** Measurement of $J_{0s}$ of Cz-Si samples passivated with a $SiO_xN_y$:H/$SiN_x$:H stack during treatment at ≈1 sun and 150 °C with (left) variation of belt speed and (right) variation of measured peak firing temperature. Part of data taken from Ref. [25].

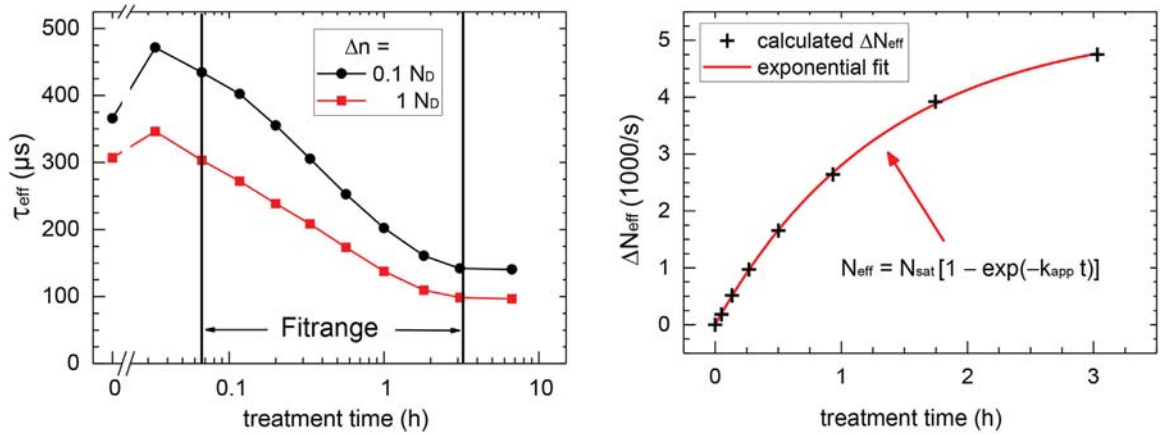


**Figure 5.** (Left) Measurement of $\tau_{eff}$ of one of the $SiO_xN_y$:H/$SiN_x$:H passivated samples used for determining $E_{app}$ during treatment at ≈1 sun and 210 °C. (Right) Values of $\Delta N_{eff}$ in a fit range as shown in the left graph. A fit with Equation (2) yields $k_{app}$. Part of data taken from Ref. [25].

evaluation at $\Delta n = 0.1 \cdot N_d$. The analysis using lifetime data at an injection level $\Delta n = N_d$ yields $E_{app} = 1.06 \pm 0.03$ eV. Changes in $\tau_b$ due to BO-LID or LeTID are known to have a greater impact at lower $\Delta n$ and thus, a potentially remaining influence of bulk degradation on the determination of $E_{app}$ should lead to a difference in the fit results at $\Delta n = 0.1 \cdot N_d$ and $\Delta n = N_d$. The good agreement of activation energy determined at two different injection levels therefore shows that the assumption of constant $\tau_b$ during SRD seems to be justified. Furthermore, the linear result of the Arrhenius plot in Figure 6 strongly suggests that the reaction leading to surface degradation is thermally activated.

Even though the empirical approach yields an apparent activation energy $E_{app}$ useful for the description of temperature dependence of SRD, it remains unclear what the meaning of this activation energy is. In the following, a more theoretical approach is described allowing for a better interpretation.

Assuming that defect formation requires a certain defect precursor and that the defect formation rate depends linearly on the concentration of this precursor, meaning one precursor converts into one defect, formation dynamics can be described by a coupled linear rate equation system

$$\frac{d}{dt} N_{prec} = -k \cdot N_{prec} = -\frac{d}{dt} N_{def} \tag{4}$$

introducing the reaction rate $k$ which represents a conversion probability from precursor to defect. For constant $k$, the solution of the equation above yields the time-dependent defect concentration

$$N_{def}(t) - N_{def}(t_0) = N_{prec}(t_0)\{1 - \exp[-k \cdot (t - t_0)]\} \tag{5}$$

The surface recombination rate $R_s$ in a sample of thickness $w$ can be described by the product of surface recombination velocity $S$ and excess charge carrier concentration $\Delta n_s$ at the surface. As dielectric passivation layers like the ones used in this study carry fixed charges that repel or attract charge carriers, $\Delta n_s$ at the actual surface differs from that in the deep bulk ($\Delta n$). For sufficiently high fixed charge densities $Q$, this effect can be taken into account by replacing $\Delta n_s$ by $c \cdot \Delta n / Q^2$ with $c$ being constant.[23] Surface recombination of a symmetrically coated sample is thus given as

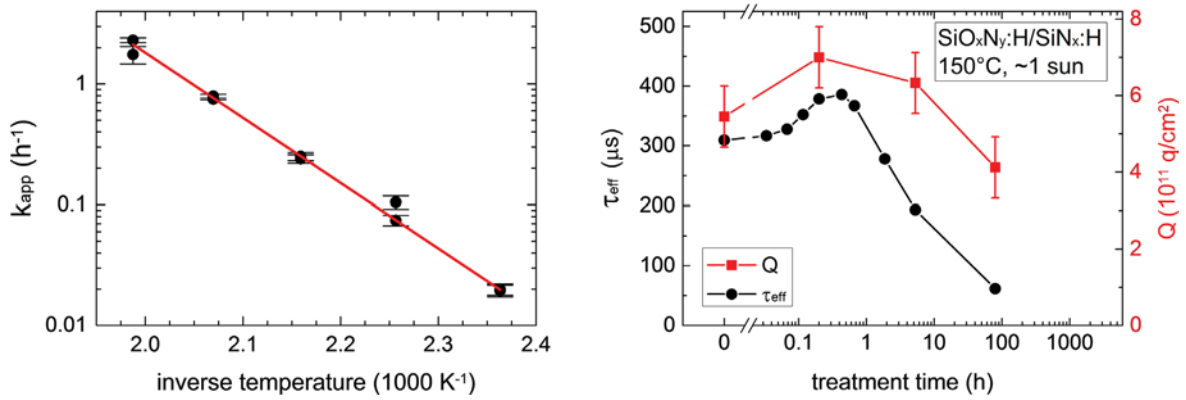


**Figure 6.** (Left) Arrhenius plot of determined degradation rates at different temperatures and $\Delta n = 0.1\, N_d$. A linear fit yields the apparent activation energy $E_{app}$. (Right) Measurement of $\tau_{eff}$ ($\Delta n = 0.1\, N_d$) and $Q$ of a Cz-Si sample passivated with $SiO_xN_y$:H/$SiN_x$:H during treatment at ≈1 sun and 150 °C. Part of data taken from Ref. [25].

$$R_s = \frac{2 \cdot S}{w} \Delta n_s = \frac{2 \cdot c \cdot S}{w \cdot Q^2} \Delta n \tag{6}$$

Total recombination $R_{tot} = \Delta n / \tau_{eff}$ is the sum of recombination $R_b$ in the bulk (bulk lifetime $\tau_b$) and $R_s$ at the surface and thus the measurable effective lifetime $\tau_{eff}$ of excess charge carriers in a sample of thickness $w$ can be approximated as

$$\frac{1}{\tau_{eff}} = \frac{R_{tot}}{\Delta n} = \frac{R_b}{\Delta n} + \frac{R_s}{\Delta n} = \frac{1}{\tau_b} + \frac{2 \cdot c \cdot S}{w \cdot Q^2} \tag{7}$$

Assuming constant $\tau_b$, the difference of inverse effective lifetimes as defined in Equation (1) then yields

$$\Delta N_{eff}(t) = \frac{2 \cdot c}{w} \left[ \frac{S(t)}{Q^2(t)} - \frac{S(t_0)}{Q^2(t_0)} \right] \tag{8}$$

Assuming in a first scenario that the fixed charge remains unchanged and $S \propto N_{def}$, Equation (8) simplifies to

$$\Delta N_{eff}(t) = \frac{2 \cdot c'}{w \cdot Q^2} [N_{def}(t) - N_{def}(t_0)] \tag{9}$$

and together with Equation (5), the equivalent defect concentration follows exactly the single exponential saturating growth function which was used in the empirical approach to fit the experimental data. In this case, the determined apparent reaction rate $k_{app}$ equals the defect formation rate $k$ and the determined activation energy corresponds to defect formation at the surface. However, capacitance–voltage measurements shown in Figure 6 (right) indicate that $Q$ changes noticeably during treatment in correlation with changes in $\tau_{eff}$. Hence, the assumption of unchanged fixed charge density in this first scenario is critical.

In a second scenario, one could argue that only the fixed charge density changes ($Q \propto N_{def}$) but that no recombination active defects form at the surface ($S$ constant). In this case, the determined activation energy relates to the recharging process. However, unlike in the first scenario, the second scenario does not produce a single exponential function for the equivalent defect density which is in contradiction to the observation that $\Delta N_{eff}$ is quite well describable by a single exponential saturating growth curve (Figure 4). Furthermore, the observed loss in fixed charge density is too small to fully explain the observed degradation in effective lifetime according to one-dimensional numeric simulations using the software PC1Dmod 6.2[31] (data not shown).

In principle, there is no reason why both extreme scenarios should not occur in parallel. One could argue that formation of defects and charged sites at the surface are one and the same process: the formed defect could not only be recombination active, but could carry a charge, leading to $S \propto N_{def}$ and $Q \propto N_{def}$. Even though $k_{app} \neq k$ in this scenario, the determined apparent activation energy $E_{app}$ relates to both the formation of defects at the surface and simultaneous charging. However, simulations using Equation (8) show that this scenario does not reproduce a single exponential saturating growth curve either.

Only in a fourth scenario, abandoning the direct correlation of defect formation and recharging by allowing two different reaction rates $k_{def}$ and $k_Q$, the observed single exponential saturating growth curve in $\Delta N_{eff}$ can be reproduced in case of changing $Q$. Unfortunately, this implies that neither determined $k_{app}$ nor $E_{app}$ are related to a single process but rather the result of a complex superposition of changes in the number of defects and density of fixed charges at the sample surface. Simultaneous changes in both parameters have been observed in $AlO_x$:H/$SiN_x$:H passivated samples before,[17] whereas in $SiN_x$:H passivated samples fixed charges remain constant and SRD appears to be caused by changes in defect density only.[16,17]

## 4. Conclusions

In summary, it has been shown that Cz-Si lifetime samples passivated by PECVD deposited layer stacks may suffer from significant bulk and surface-related degradation already at relatively low temperatures of 80 °C under illumination in ambient air. Significant differences in bulk-related degradation are probably linked to a different impact of LeTID in differently passivated samples. A closer investigation of surface-related degradation in $SiO_xN_y$:H/$SiN_x$:H passivated samples yields an apparent activation energy of $E_{app} = 1.07 \pm 0.02$ eV which is useful for the empirical description of temperature dependencies. However, as both chemical passivation (defects at the surface) and field effect passivation (fixed charges in the dielectric layer) are assumed to deteriorate in parallel, this apparent activation energy can neither be unambiguously related to the formation of defects at the surface nor the formation/annihilation of charged sites in the dielectric layer. Additionally, further studies are needed to clarify to what extent SRD affects solar cells under real operation conditions in the field.


## Acknowledgments

D.S., A.S., and A.H. contributed equally to this work. The authors would like to thank A. Graf, L. Mahlstaedt, F. Mutter, B. Rettenmaier, S. Joos, and J. Engelhardt for technical support. Part of this work was supported by the German Federal Ministry for Economic Affairs and Energy under contract numbers 0324204B and 0324001. The content is the responsibility of the authors.


## Conflict of Interest

The authors declare no conflict of interest.


## Keywords

Czochralski, LeTID, light-induced degradation, PECVD, surface-related degradation

[1] J. Lindroos, H. Savin, *Sol. Energy Mater. Sol. Cells* **2016**, *147*, 115.
[2] H. Fischer, W. Pschunder, in *Proc. 26th IEEE Photovolt. Spec. Conf. Rec.*, Palo Alto, USA **1973**, p. 404.
[3] J. Schmidt, A. Aberle, R. Hezel, in *Proc. 26th IEEE Photovolt. Spec. Conf. Rec.*, Anaheim, USA **1997**,p. 13.
[4] S. W. Glunz, S. Rein, W. Warta, J. Knobloch, W. Wettling, in *Proc. 2nd World Conf. Photovolt. Energy Conver.*, Vienna, Austria **1998**, p. 1343.
[5] T. Niewelt, J. Schön, W. Warta, S. W. Glunz, M. C. Schubert, *IEEE J. Photovolt.* **2017**, *7*, 383.
[6] B. Hallam, A. Herguth, P. Hamer, N. Nampalli, S. Wilking, M. Abbott, S. Wenham, G. Hahn, *Appl. Sci.* **2017**, *8*, 10.
[7] G. Zoth, W. Bergholz, *J. Appl. Phys.* **1990**, *67*, 6764.
[8] D. H. Macdonald, L. J. Geerligs, A. Azzizi, *J. Appl. Phys.* **2004**, *95*, 1021.
[9] L. J. Geerligs, D. Macdonald, *Appl. Phys. Lett.* **2004**, *85*, 5227.
[10] K. Ramspeck, S. Zimmermann, H. Nagel, A. Metz, Y. Gassenbauer, B. Birkmann, A. Seidl, in *Proc. 27th Eur. Photovolt. Sol. Energy Conf. Exhib.*, Frankfurt/Main, Germany **2012**, p. 861.
[11] F. Fertig, K. Krauß, S. Rein, *Phys. Status Solidi RRL* **2015**, *9*, 41.
[12] F. Kersten, P. Engelhart, H. C. Ploigt, A. Stekolnikov, T. Lindner, F. Stenzel, J. W. Müller, *Sol. Energy Mater. Sol. Cells* **2015**, *142*, 83.
[13] F. Fertig, R. Lantzsch, A. Mohr, M. Schaper, M. Bartzsch, D. Wissen, F. Kersten, A. Mette, S. Peters, A. Eidner, J. Cieslak, K. Duncker, M. Junghänel, E. Jarzembowski, M. Kauert, B. Faulwetter-Quandt, D. Meißner, B. Reiche, S. Geißler, S. Hörnlein, C. Klenke, L. Niebergall, A. Schönmann, A. Weihrauch, F. Stenzel, A. Hofmann, T. Rudolph, A. Schwabedissen, M. Gundermann, M. Fischer, J. W. Müller, D. J. W. Jeong, *Energy Procedia* **2017**, *124*, 338.
[14] D. Chen, M. Kim, B. V. Stefani, B. J. Hallam, M. D. Abbott, C. E. Chan, R. Chen, D. N. R. Payne, N. Nampalli, A. Ciesla, T. H. Fung, K. Kim, S. R. Wenham, *Sol. Energy Mater. Sol. Cells* **2017**, *172*, 293.
[15] D. Sperber, A. Herguth, G. Hahn, *Sol. Energy Mater. Sol. Cells* **2018**, *185*, 277.
[16] D. Sperber, A. Graf, D. Skorka, A. Herguth, G. Hahn, *IEEE J. Photovolt.* **2017**, *7*, 1627.
[17] D. Sperber, A. Schwarz, A. Herguth, G. Hahn, *Sol. Energy Mater. Sol. Cells* **2018**, *188*, 112.
[18] B. Veith-Wolf, R. Witteck, A. Morlier, H. Schulte-Huxel, M. R. Vogt, J. Schmidt, *IEEE J. Photovolt.* **2018**, *8*, 96.
[19] M. A. Green, *Sol. Energy Mater. Sol. Cells* **2015**, *143*, 190.
[20] A. Herguth, C. Derricks, D. Sperber, *IEEE J. Photovolt.* **2018**, *8*, 1190.
[21] A. Herguth, *Energy Procedia* **2017**, *124*, 53.
[22] R. A. Sinton, A. Cuevas, M. Stuckings, in *Proc. 25th IEEE Photovolt. Spec. Conf. Rec.*, Washington D.C., USA **1996**, p. 457.
[23] K. R. McIntosh, L. E. Black, *J. Appl. Phys.* **2014**, *116*, 014503.
[24] A. Kimmerle, J. Greulich, A. Wolf, *Sol. Energy Mater. Sol. Cells* **2015**, *142*, 116.
[25] A. Schwarz, *Bachelor Thesis*, University of Konstanz, September **2017**.
[26] T. Niewelt, W. Kwapil, M. Selinger, A. Richter, M. C. Schubert, *IEEE J. Photovolt.* **2017**, *7*, 1197.
[27] C. Vargas, K. Kim, G. Coletti, D. Payne, C. Chan, S. Wenham, Z. Hameiri, *IEEE J. Photovolt.* **2018**, *8*, 413.
[28] J. Fritz, A. Zuschlag, D. Skorka, A. Schmid, G. Hahn, in *Proc. 33rd Eur. Photovolt. Sol. Energy Conf. Exhib.*, Amsterdam, The Netherlands **2017**, p. 569.
[29] K. Nakayashiki, J. Hofstetter, A. E. Morishige, T. T. A. Li, D. B. Needleman, M. A. Jensen, T. Buonassisi, *IEEE J. Photovolt.* **2016**, *6*, 860.
[30] D. Bredemeier, D. Walter, S. Herlufsen, J. Schmidt, *AIP Adv.* **2016**, *6*, 035119.
[31] H. Haug, J. Greulich, *Energy Procedia* **2016**, *92*, 60.